Respiratory Physiology & Neurobiology 265 (2019) 161–171

Contents lists available at ScienceDirect

Respiratory Physiology & Neurobiology

journal homepage: www.elsevier.com/locate/resphysiol

Ventilatory pattern variability as a biometric for severity of acute lung injury in rats

Benjamin P. Young[a], Kenneth A. Loparo[b], Thomas E. Dick[a,c,*], Frank J. Jacono[a,d]

[a] Division of Pulmonary, Critical Care, & Sleep Medicine, Department of Medicine, School of Medicine, Case Western Reserve University, Cleveland, OH 44106, USA
[b] Department of Electrical Engineering and Computer Science, School of Engineering, Case Western Reserve University, Cleveland, OH 44106, USA
[c] Department of Neurosciences, School of Medicine Case Western Reserve University, Cleveland, OH 44106, USA
[d] Division of Pulmonary, Critical Care and Sleep Medicine, Department of Medicine, Louis Stokes VA Medical Center, Cleveland, OH 44106, USA

ARTICLE INFO

Keywords:
Neural control of respiration
Biometrics of respiratory disease
Nonlinear dynamics
Brainstem inflammation

ABSTRACT

We hypothesize that ventilatory pattern variability (VPV) varies with the magnitude of acute lung injury (ALI). In adult male rats, we instilled a low- or high- dose of bleomycin or saline (PBS) intratracheally. While representative samples of pulmonary tissue indicated graded lung injury, coefficient of variation (CV) of TTOT did not differ among the 3 groups. Broncho-alveolar lavage fluid (BALF), respiratory rate (fR), mutual information were greater in ALI than sham rats; but did not differ between bleomycin doses. However, nonlinear complexity index (NLCI), which is the difference in sample entropy between original and surrogate data sets was greater for high- versus low- dose; but did not differ between low-dose and sham groups. Further, NLCI correlated to an injury index based on protein concentration of BALF and failure to gain weight. Finally, Receiver Operator Curves (ROCs) indicated that both mutual information and NLCI had greater sensitivity and specificity than fR and CVTTOT in identifying ALI. Thus, nonlinear analyses of VPV can distinguish ALI and out performs fR as a biometric.

1. Introduction

Our diverse group has a common interest in understanding ventilatory pattern variability (VPV). While variable breathing patterns are associated with morbidity (Tobin, 1992; Tobin et al., 1983a,b), measuring the variability as the mean, standard deviation and coefficient of variation (CV) of cycle duration cannot distinguish patterns that are ataxic like Biot's breathing from ones that are periodic like Cheyne-Stokes pattern. We theorized that a measure of variability that can distinguish linear (random) from non-linear (time-dependent) factors would be valuable clinically. In other words, current measures of respiratory variability evaluate each breath as an independent entity and focus on respiratory frequency (fR); whereas we are examining variability of a pattern both its frequency and waveform, and how the next breath depends on previous breaths in a series of breaths.

Over the last decade, we have developed analytical tools that assess the variability of continuous respiratory waveforms, such as those recorded by whole-animal, flow-through plethysmography to integrated motor activities (Dhingra et al., 2011; Dick et al., 2013; Jacono et al., 2011). We refer to our analytical approach as VPV to distinguish it from an approach that assesses only variations in respiratory phase-switching and cycle duration. Our general working hypothesis is that assessing VPV is a biometric that reflects health status. We theorized that our metric should evaluate the respiratory system particularly the function of the ponto-medullary neural circuit that generates the respiratory pattern and test our analytic approach on a preclinical model of acute lung injury.

Acute lung injury (ALI) and acute respiratory distress syndrome (ARDS) are characterized by a severe inflammation of the lung that damages alveolar epithelial and endothelial barriers increasing: pulmonary vascular permeability, pulmonary edema, poorly aerated lung tissue and infiltrates of eosinophils and macrophages in the alveoli (Atabai and Matthay, 2002). ALI and ARDS remain associated with substantial mortality (44% mortality between 1994–2006 (Phua et al., 2009)) despite advances in supportive care including neuromuscular blockade and prone positioning, as well as lung-protective ventilatory strategies (Phua et al., 2009). Effective biometrics would identify clinical features early, provide risk stratification, reflect responses to therapy and predict outcomes. We have used our analytical approach to identify changes in VPV early in ALI (Jacono et al., 2011). Here, we test

* Corresponding author at: Division of Pulmonary, Critical Care and Sleep Medicine, Department of Medicine, Case Western Reserve University School of Medicine, 11000 Euclid Avenue, Cleveland, OH, 44106-5067, USA.
E-mail address: ted3@case.edu (T.E. Dick).

https://doi.org/10.1016/j.resp.2019.03.009
Received 20 April 2018; Received in revised form 5 March 2019; Accepted 26 March 2019
Available online 27 March 2019
1569-9048/

its ability to identify ALI 7d after injury when the inflammatory response peaks, to determine if nonlinear measures vary with the magnitude of lung injury and to compare the sensitivity of our measures to fR.

1.1. Heart rate variability (HRV)

For approximately a half century, cardiologists have tested and used analytical tools of HRV for their diagnostic and prognostic value (Malik, 1996). Analytic approaches examine HRV in both temporal and frequency domains and assess linear and nonlinear properties of HRV. Nonlinear analyses examine predictability of patterns (Hoyer et al., 1997; Kurths et al., 1995; Voss et al., 1995). In a recent publication, we analyzed HR dynamics using a multiscale entropy algorithm, then plotted values in a physiologic, pathophysiologic state space reflecting the health-disease continuum (Vandendriessche et al., 2017). Thus, tracking biometrics is a strong rationale underlying their use as clinical tools especially in the context of Intensive Care Unit where patient's electrocardiogram and other physiologic signals are monitored for days.

1.2. Ventilatory pattern variability (VPV)

The variation in breathing pattern does not have the extensive history of HRV, but a clinical study compared measures of HRV and fR variability (fRV) during spontaneous breathing trials to determine if HRV and fR could predict extubation failure in ventilated patients (Seely et al., 2014). While changes in HRV predicted extubation failure, a predictive model using fRV had better accuracy than one based on HRV (Seely et al., 2014). Their report focused on changes in frequencies of respiratory and the cardiac cycles and found that fRV was a better biometric than HRV in weaning from a ventilator.

1.3. Rationale for methodologic approach

We view ventilation as a continuous oscillatory waveform, which has both a rhythm and a pattern. This distinction emphasizes that the waveform has not only a rate and magnitude, but also a shape and predictability from cycle to cycle. We use surrogate data sets designed to preserve the linear properties of the original data set and to disrupt its nonlinear, time- and pattern- dependent properties (Schreiber and Schmitz, 2000, 1996).

The respiratory pattern is generated by a brainstem neural network, which integrates sensory and central information. In the development and progression of ALI, we expect that activation of vagal pulmonary sensory nerves and changes in pulmonary mechanics will be reflected in alterations in respiratory motor activities and, ultimately, ventilatory pattern. We and others have theorized that fundamental changes in waveform include the consistency or variability of the pattern (Goldberger et al., 2002a, 2002b; Papaioannou et al., 2011; Peng et al., 2002). Thus, VPV changes can reflect the development of disease (Jacono, 2013).

In a previous study, we recorded the ventilatory pattern at 6, 12, 24 and 48 h after ALI, and reported that at 24 and 48 h, VPV and fR were greater in ALI versus sham preparations (Jacono et al., 2011). We theorized the increased fR did not depend solely on peripheral feedback from the lungs, because pro-inflammatory cytokines were present in cardiorespiratory nuclei in the brainstem at the following ALI. We associated the persistent increased fR and variability to cytokines affecting the respiratory central pattern generator and/or its sensory input.

In this report, we applied analytical tools to quantify VPV as a technique to assess disease severity in a rodent model of ALI 7d after the insult. We hypothesize that as severity of the injury increased; the inflammatory response would increase and the respiratory system would become constrained; and VPV would become more deterministic. In effect the next breath would become more predictable.

Therefore, we measured ventilation after the development of ALI, quantified the underlying structure of the variability of the breathing pattern and associated changes in VPV with severity of lung injury. We expanded beyond the traditional analyses of respiratory intervals (that is, respiratory rate and duration of the respiratory cycle) to include assessment of the shape and patterning of the respiratory waveform. In addition, we applied metrics of nonlinear complexity to determine if changes in nonlinear measures of VPV would be a better predictor of the presence of lung injury than the standard linear measures of respiratory variability (i.e., coefficient of variation of respiratory rate).

2. Materials and methods

2.1. Surgical and experimental procedures

Experiments were performed on young adult, male Sprague Dawley (Harlan Laboratories) rats (n = 26) weighing between 120–200 g. The Institutional Animal Care and Use Committee of Case Western Reserve University approved the experimental protocols.

2.1.1. Induction of lung injury

General surgical anesthesia was established with ketamine, xylazine, and acepromazine utilizing a weight-based dose injected intraperitoneally as described previously (Jacono et al., 2011). Briefly, we placed the anesthetized rat supine, exposed the trachea, inserted a 26-gauge needle between cartilaginous rings of the trachea and injected phosphate-buffered saline (PBS (50 µl) n = 9 rats) or low- or high- dose bleomycin (bleomycin) [1 unit in 50 µl (n = 9 rats) or 3 units in 150 µl of PBS (n = 8 rats)]. The incision was sealed with surgical tissue adhesive and rats were monitored during recovery.

2.1.2. Ventilatory measurements

Whole-body plethysmography: Ventilation was recorded from unanesthetized, unrestrained, spontaneously breathing rats using a flow-through, whole-body plethysmograph (Model PLY4213, Buxco Electronics, Inc., Wilmington, NC). Briefly, this system has two chambers; an animal and a reference chamber, and the pressure difference between the chambers is recorded. During inspiration the increased temperature and humidity of the air in the rat's lungs causes a slight increase in pressure in the plethysmograph (Delorme and Moss, 2002; Lundblad et al., 2002; Nirogi et al., 2012). The animal chamber has gas in and out ports for continuous flow (1.75 l/min) of gas through the chamber to prevent depletion of O_2 and accumulation of CO_2 during the recording period. The reference chamber is connected to the animal chamber via a high-resistance port to allow compensation for slow shifts in pressure between the chambers.

Prior to placing a rat in the animal chamber, we calibrated the voltage evoked with a pressure difference by injecting and withdrawing 0.5 ml of air in and out of the animal chamber at 2–3 Hz, approximately a rat's respiratory rate. After placing a rat in the plethysmograph, it was allowed 30 min to acclimatize to the chamber before the signal was recorded and stored in a computer using commercial acquisition software (Spike2 v6, Cambridge Electronic Design Limited, Cambridge, England). Data were analyzed 'off-line'. Plethysmographic pressure was conditioned (Filter settings: 0.1–30 Hz) and sampled at 200 Hz. Recordings were obtained at an ambient room temperature of 24 ± 1 °C and between 9 A M and 1 PM to minimize circadian effects on the results. Baseline respiratory parameters were collected for 10 min with the rat breathing normoxia (room air, 21% O_2 - 79% N_2). Subsequently, ventilatory responses to hyperoxia (5 min, 100% O_2), and hyperoxic hypercapnia (95% O_2 - 5% CO_2) were obtained. Breathing patterns were recorded at day 0 (before lung injury) and day 7, which was 1 week after intra-tracheal administration of either bleomycin or vehicle.

2.2. Assessment of lung injury and inflammation

2.2.1. Collection of bronchoalveolar lavage fluid (BALF)

After the plethysmographic recording on day 7, rats were anesthetized and exsanguinated. A midline incision extending from the thorax to the neck was made, the ventral ribs were removed to allow unencumbered lung expansion, and the trachea was cannulated. The lungs were lavaged with sterile PBS (3 times, 3 ml each time). The collected bronchoalveolar lavage fluid (BALF) was centrifuged (1500 *g*, 10 min at 4 °C) and the supernatant was collected for protein analysis.

2.2.2. BALF protein assay

Protein content of BALF was determined using a modified Bradford Protein Assay (Bio-Rad Laboratories, Hercules, CA). Briefly, 5 ml of diluted dye reagent was added to 100 µl of BALF supernatant and mixed. Dye-protein complexes were formed during a 10-min incubation at room temperature and were analyzed spectrophotometrically at 595 nm. Protein concentration was determined by comparison to a standard curve constructed using known amounts of bovine serum albumin. The results are expressed as µg of protein per µl of BALF.

2.2.3. Pulmonary histology

Lungs from euthanized rats (n = 2 in each group and BALF was not collected from these rats) were inflated and fixed with 10% formalin at 25 cmH_2O for 30 min. The lungs were removed *en bloc*, transferred to a cassette, and embedded in paraffin. Subsequently, 5-µm sections were cut and stained with hematoxylin and eosin for histological examination.

2.2.4. Weight

We weighed the rats on days 0 - 7. Vehicle-sham rats gained weight whereas rats with ALI gained less or lost weight in the most severely injured. Generally, visual inspection of the rat correlated with its well-being. For example, rats minimally affected by the intratracheal injections of bleomycin were mobile and active, had a groomed hair coat, had clear eyes and gained weight; whereas those affected, were hunched and stationary, had a rough hair coat, had serous discharge from their eyes and lost weight (Kohn et al., 2007).

2.2.5. Injury index

We devised an objective index of the severity of injury based on a rat's inability to gain weight which was the rat's actual weight subtracted from an expected weight determined by the weight gain of the sham injury group and on the protein concentration of the BALF.

2.3. Data analysis

The assessment of VPV among experimental groups of rats was conducted using a complementary set of novel analytical tools to quantify changes in the morphology of the breathing pattern (Dhingra et al., 2011). Stationary (without sighs or abrupt changes in pattern), artifact-free epochs (60 s duration) were identified for analysis from the recorded respiratory signal, and a video recording of the rat. Epochs were scored using breath-detection software (Case Western Reserve University, Cleveland, OH).The analysis of phase durations and respiratory rate consisted of determining the mean, standard deviation and co-efficient of variation for each variable. These statistics determine the distribution and regularity of the temporal components or 'rhythm' of respiration but do not evaluate other sources of variability in the ventilatory motor pattern. To characterize ventilatory pattern variability, we conducted a time series analysis on the raw signal, as well as on surrogate data sets formed from the raw signal. This analysis included autocorrelation function, mutual information and sample entropy.

2.3.1. Autocorrelation

Autocorrelation (AC) functions were constructed to characterize the linear relationship between sampled points in the pattern. For each breathing epoch, AC was calculated using available MATLAB (Mathworks, Natick, MA) routines across multiple time intervals or lags (τ) from neighboring points to points separated by one respiratory cycle length (TTOT). To facilitate comparisons across rats with different respiratory rates, the value of the AC coefficient at one respiratory cycle length was reported as a measure of the strength of linear correlations for a time series.

2.3.2. Mutual information

Mutual information (MI) is a measure of statistical dependence in the data set that quantifies the reduction in the amount of uncertainty of a point at time-delay $x(t+\tau)$ by knowledge of the point at $x(t)$. MI was computed for each τ between 1 and 1-cycle length. We reported an average value for MI, excluding the first and last 17.5% of the cycle, thus limiting those values that are near to and approximately a cycle length from the reference value, because of the strong linear correlations as defined by the AC function. MI was calculated for both original and surrogate data sets to detect the presence of nonlinear dependence over a physiologically appropriate range of time-delays. Specifically, if there is nonlinear information in the original epoch its MI should be statistically higher than the MI of the surrogate data (Dhingra et al., 2011; Weil et al., 2009).

2.3.3. Sample entropy

Sample Entropy (SampEn) is a measure of the predictability of a time-series signal (Richman and Moorman, 2000). To calculate sample entropy, a template of m ($m = 2$ for our analysis) points is selected and the entire epoch is searched for template matches within a certain tolerance r ($r = 0.2$*SD), let this value be A. The procedure is repeated with a template of $m+1$ (m = 3) points, let the number of such matches be equal to B. SampEn is defined as ln(A/B) where self-counting is eliminated. Computationally, SampEn is the negative natural logarithm of the conditional probability that epochs of a certain length having a certain number of matches within a tolerance r for m number of points will also have matches for $m + 1$ points within the same r where r is a percentage of the amplitude maximum for a given epoch (Dhingra et al., 2011). In addition, a modified SE method was utilized incorporating time delays other than unity to quantify contributions to pattern complexity across time scales relevant to the respiratory cycle length (Kaffashi et al., 2008).

2.3.4. Surrogate data & nonlinear complexity index (NLCI)

We applied this technique to distinguish linear versus nonlinear sources of variability in the plethysmographic signal (Dhingra et al., 2011). Surrogate datasets (n = 19) were computed using the iterated amplitude adjusted Fourier transform (iAAFT) by moving the data into the frequency domain and back into the time domain while ensuring that both the frequency distribution (power spectrum/autocorrelation function) and the amplitude distribution are maintained (Fig. 1). These surrogate data sets are designed to preserve the linear correlations while disrupting nonlinear, time-dependent, relationships in the signal (Dhingra et al., 2011; Schreiber and Schmitz, 2000, 1996).

These data are plotted against τ, which is the time delay or interval between sampled points in the signal. τ ranged from 1 to 1 cycle length. The differences between mutual information or sample entropy of the surrogates and original data sets are used as an index of the amount of nonlinear complexity present in the data for a given value of τ (Dhingra et al., 2011; Schreiber and Schmitz, 2000, 1996)

As stated, nonlinear contributions were explored by comparing the SampEn of the original data set from those of the surrogate data sets (Kaffashi et al., 2008). SampEn was computed over multiple τs from one to one cycle length for both original and surrogate data sets. We report SampEn like MI averaging the values in the middle 65% of the

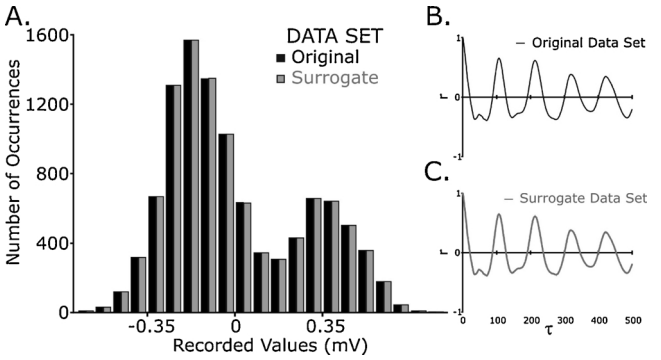

Fig. 1. Representative examples of original and surrogate data sets. **A1** Black tracing: an original recording from the plethysmograph (specifically from a rat treated with PBS, the vehicle for bleomycin, breathing normoxia). **A2** Gray tracing: surrogate data generated from the original data. **B** Distribution of values for the amplitude of the waveforms of the original (black) and surrogate (gray) data sets. The surrogate data replicates the amplitude distribution of the original data. **C1** Black tracing: The autocorrelation function of the original data plotted against τ (τ = 1 to 4 cycles). **C2** Gray tracing: Surrogate data sets were selected because their autocorrelation function matched within tolerance that of the original data.

curve due to the effect of the strong linear correlations at τ near 1 and at 1-cycle length.

To further determine complexity attributable to nonlinear features, differences were tabulated between SampEn for original and surrogate datasets at each individual τ. A nonlinear complexity index (NLCI) was computed by taking the sum of absolute values of all statistically significant differences in sample entropy between the surrogate and original data sets divided by the number of 'τ's included in the sum. Greater values of the NLCI correlate with increased contributions of nonlinear and linear non-Gaussian sources of variability (Seely and Macklem, 2004; Dhingra et al., 2011).

3. Results

3.1. Lung injury by bleomycin

3.1.1. Lung histology and BALF

The extent of lung injury was examined 7d after intra-tracheal administration of either PBS or bleomycin (Fig. 2). Lung histology revealed that alveolar architecture remained intact in the lungs of the PBS-treated rats (Fig. 2A) but was damaged in bleomycin-treated rats (Fig. 2B and C). Damage varied; and inflammatory cells infiltrated to damaged areas indicating an inflammatory response following low- and high- dose bleomycin (Fig. 2B and C).

We measured BALF protein concentration as an index of alveolar-capillary permeability, which increases with lung injury (Fig. 2D) and with the severity of lung injury (Fig. 2E). The average BALF protein concentration was 0.02 ± 0.01 μg/μl for the Sham group (n = 7 rats); 0.13 ± 0.1 μg/μl, (n = 7) for low-dose; and 0.21 ± 0.20 μg/μl, (n = 8) for high-dose bleomycin groups. The average BALF protein concentrations of the low- and high- dose bleomycin groups were greater than that of the sham group ($P < 0.05$) but were not significantly different from each other (Fig. 2D). Bleomycin causes focal lung injury isolated to the areas of its deposition. This leads to a mottled rather than homogenous lung injury. The broad distribution of protein concentrations of the BALF also indicated variation in the extent of lung injury.

3.1.2. Weight gain and BALF

The mean ± SD changes in weight for the three groups were: the sham group, 49 ± 7.0 g; the low-dose bleomycin group, 16 ± 18.3 g and the high dose, -10 ± 32.8 g. The large standard deviations for the means in the change in body weight in the rats receiving bleomycin was similar to those observed with BALF. To assess the potential range of lung injury with bleomycin, we plotted the change in weight from d0 to d7 against the BALF protein concentration value on d7 and identified each point as receiving PBS or 1U or 3U of bleomycin (Fig. 2E). It was apparent that: 1) 3 rats (2 received 1U and 1 received 3U of bleomycin) had mild lung injury with weight gain and BALF protein concentration similar to the group of PBS-treated rats, 2) 2 rats that received 3U of bleomycin had the greatest weight loss and highest concentrations of protein in their BALF so had the most severe lung injury, and 3) 8 rats (5 received 1U and 3 received 3U of bleomycin) were between these extremes and had a wide distribution of values(Fig. 2E). We present our the data based on the dose of bleomycin the rats received bu include an assessment of our analytical tools against the severity of injury as indicated by the change in body weight multiplied by the BALF protein concentration.

3.2. Impact of lung injury on breathing pattern

Representative respiratory tracings from a rat in each exposure group are shown in Fig. 3A, left column with the corresponding cycle-triggered averages (CTAs) of the tracing shown in Fig. 3A, right column. Averaging was triggered at zero, *e.g.*, when airflow crossed from negative (expiration) to (positive) inspiration. This increased the signal-to-noise ratio of the plethysmographic signal and revealed the underlying change in the ventilatory pattern (Fig. 3A, right column). Qualitative assessment of the CTAs suggested that the respiratory pattern became more similar to a sine wave after lung-injury compared to sham treatment. In particular, pattern variability that was expressed as oscillations or 'ripples' during inspiration and late expiration in PBS-treated rats diminished progressively after lung injury.

3.2.1. Respiratory frequency (fR)

Lung injury increased fR (Fig. 3). In unanesthetized rats breathing room air, respiratory rate (fR) was slower in PBS- compared to bleomycin- treated rats (fR = 100 ± 8 breaths/min in the PBS-treated group (n = 9); 191 ± 81 breaths/min (n = 9; $P < 0.05$) in the low-dose and 206 ± 78 breaths/min (n = 8; $P < 0.01$) in the high-dose bleomycin-treated group (Fig. 3B). The difference in fR between the low- and high-dose bleomycin-exposed rats was not significant ($P = 0.72$).

3.2.2. Coefficient of variation (CV)

We calculated the coefficient of variation (CV) of cycle length (TTOT) to assess total variability in the timing of the respiratory cycle. Comparing to d7, the means (± SD) of CVTTOT were: 1) for the PBS group, 0.13 ± 0.03 at d0 and 0.13 ± 0.04 at d7 (n = 9); 2) for the low-dose group, 0.14 ± 0.05 at d0 and 0.30 ± 0.21 (n = 9), and 3) for the high-dose group, 0.21 ± 0.20 at d0 and 0.41 ± 0.20 at d7 (n = 8). Similar to fR, CVTTOT increased in the rats that received bleomycin compared to those that received PBS but the bleomycin-treatment groups did not differ from each other (Fig. 3C).

In summary, fR increases with induction of lung injury and qualitative differences were apparent in the shape of the respiratory pattern especially with the CTAs. CVTTOT increased from d0 to d7 in the groups receiving 1 and 3U of bleomycin. Thus, variation in cycle duration across breaths in an epoch were significant in the bleomycin-treatment groups compared to the sham group, even though the bleomycin groups included rats with mild lung injuries

3.3. Effect of lung injury on ventilatory pattern variability (VPV)

In addition to measuring variation in the time domain (mean, standard deviation of fR and CVTTOT), we measured variation in the waveform produced by airflow across a pneumotach attached to the plethysmograph. We refer to these measures as ventilatory pattern

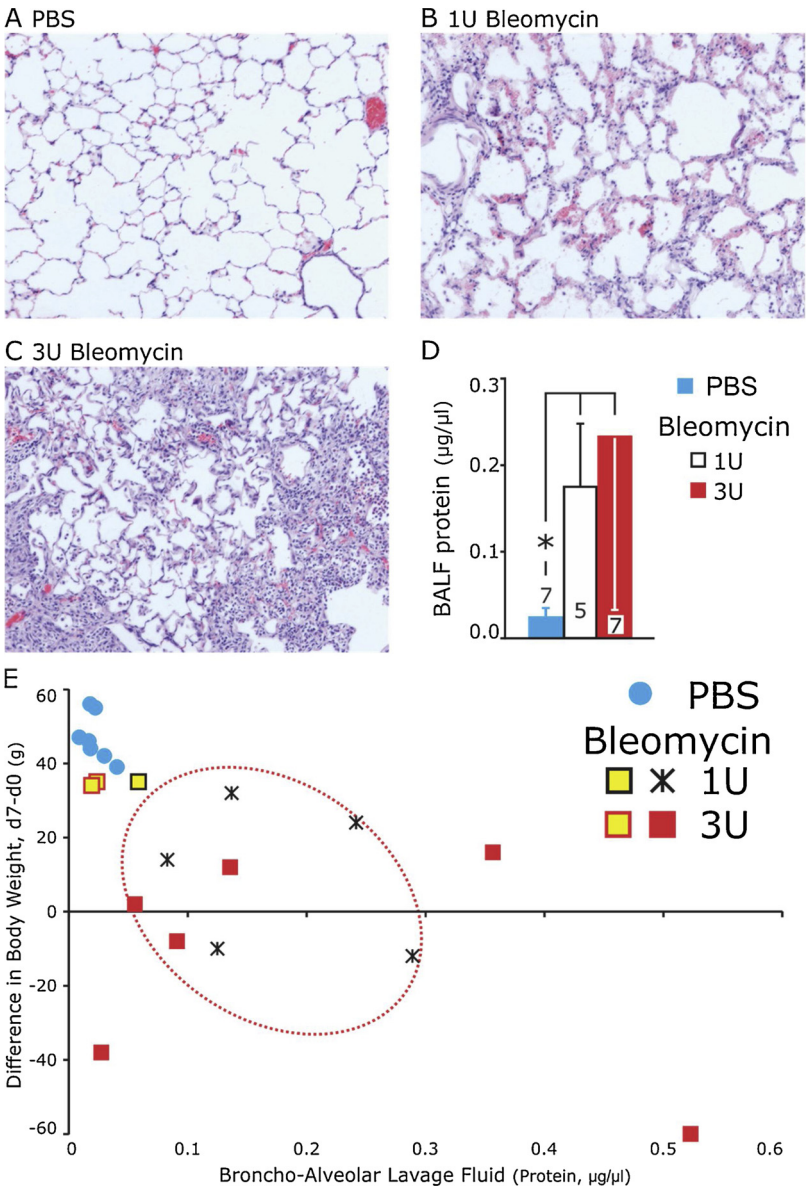

Fig. 2. We characterized lung injury by histology, protein concentration in broncho-alveolar lavage fluid (BALF) as measured on d7 and changes in body weight between d0 and d7. **A-C:** Lungs were harvested from 2 rats in each group, sectioned and stained with hematoxylin and eosin. Representative paraffin sections of pulmonary tissue exposed to, PBS (**A**); low- (**B**, 1U) and high- (**C**, 3U) dose bleomycin. Sections of pulmonary tissue from lung exposed to bleomycin had evidence of injury with inflammatory cellular infiltrates in the alveoli. **D:** The means of the protein content of BALF from low- and high- dose Bleomycin-treated rats were greater than that from PBS-treated rats (* = $P > 0.05$) but were not significantly different from each other. **E:** Plot of change in body weight against BALF protein content for each rat (coded for treatment) revealed that: 1) 3 rats that received bleomycin had similar weight gains and BALF protein content as the PBS-treated rats indicating mild lung injury, 2) 3 rats that received 3U bleomycin had the greatest weight loss and highest BALF protein concentration indicating severe lung injury; 3) 5 rats that received 1U and 3, that received 3U of bleomycin had overlapping and widely distributed changes in body weight and protein concentration in BALF (points encircled with dashed in red line), which indicated moderate lung injury. Bleomycin damages only the lung tissue, which it contacts directly resulting in mottled rather than homogenous lung injury.

variability (VPV), which was quantified using a set of complementary tools (Fig. 4) as described in 2. METHODS, 2.3 *Data Analysis*.

3.3.1. *Autocorrelation coefficients (r)*

On d0 prior to intratracheal instillation of PBS or bleomycin, the values of r at one cycle length were not significantly different among the groups: for the sham group, $r = 0.73 \pm 0.07$; for low- and high-doses of bleomycin, (0.75 ± 0.09, 0.71 ± 0.11 respectively). Even though r tended to increase a week following treatment, it did not distinguish groups: sham, $r = 0.72 \pm 0.07$; low-dose, 0.78 ± 0.05; and high-dose, 0.77 ± 0.07.

3.3.2. *Mutual information (MI) and sample entropy (SampEn)*

The results of the nonlinear deterministic analysis for the representative respiratory tracings are shown in Figures 4A&B. The predictability of the breathing pattern was evaluated by calculating the mutual information (MI) during stable breathing when the rats were quiescent (Fig. 4A1 & B1). To have a single number represent MI, we averaged the values of MI over middle 65% of τ (red horizontal lines from 17.5% to 82.5% in Fig. 4A1). The mean MIs of the original data sets were greater than the surrogate data sets for all the groups ($P < 0.01$; not shown in Fig 4A1 for clarity), at d7, the mean values of MI were greater ($P < 0.05$) for the bleomycin-treated groups (low dose, 0.74 ± 0.08 bits n = 9; high dose, 0.75 ± 0.07 bits, n = 8) compared to the Sham group (0.47 ± 0.08 bits, n = 9). The difference in the mean MIs between low- and high- dose was not significantly different. The mean MI of the surrogate data sets was greater for the low-dose bleomycin group compared to the PBS group (0.51 ± 0.05 bits, n = 9 vs. 0.39 ± 0.06 bits, n = 9; $P = 0.02$).

We quantified the linear and nonlinear property of entropies of ventilatory waveform predictability by calculating the Sample Entropy (SampEn) (Fig. 4A2 & B2). Again, to have a single number represent SampEn, we averaged the values of SampEn over middle 65% of τ (red horizontal lines in from 17.5% to 82.5% Fig. 4A2, Note the cycles were normalized to one cycle length on the x-axis so 1 red line represented the averaged section in the 3 traces).The mean SampEn of the original data sets were less than the surrogate data sets for all the groups ($P < 0.01$; not shown in Fig 4A2 for clarity). At d7, the mean value of SampEn was less ($P < 0.05$) for the lung-injured groups (low dose, 1.17 ± 0.17 bits n = 9; high dose, 1.14 ± 0.07 bits, n = 8) compared to the sham rats (1.31 ± 0.11 bits, n = 9). The difference in the mean SampEn between low- and high- dose did not differ significantly. The

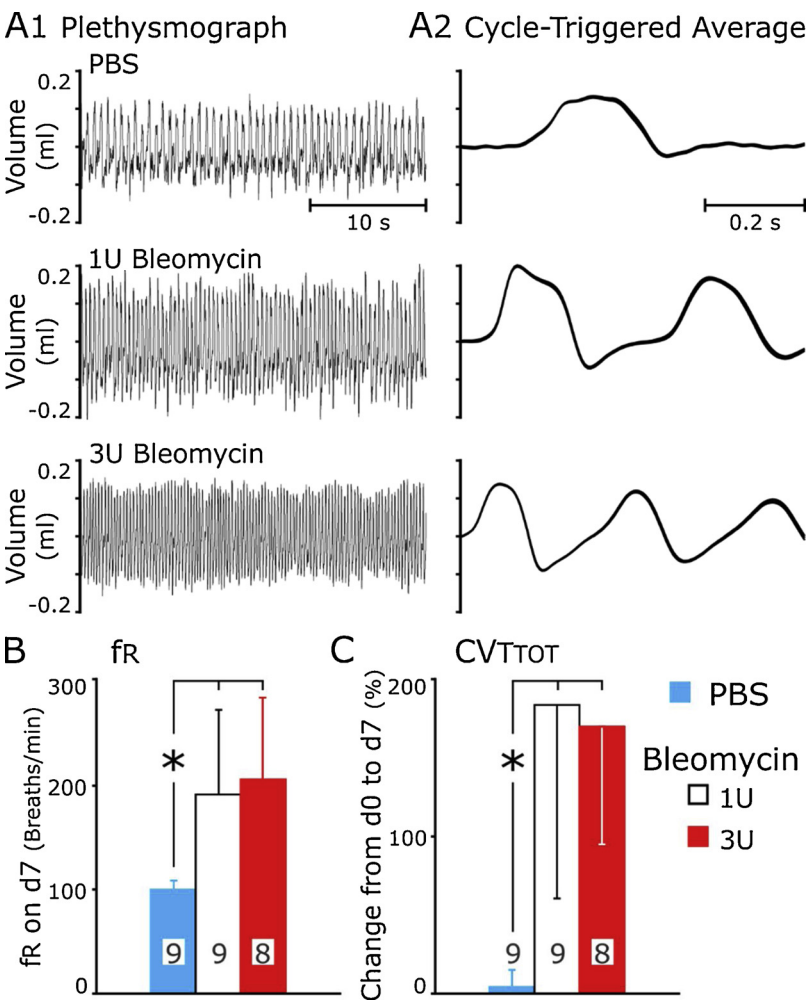

Fig. 3. Breathing patterns 7d after either receiving PBS or bleomycin. **A1** Raw traces from plethysmographic chambers in which rats breathed room air 7d after intra-tracheal instillation of PBS (vehicle) or bleomycin (low- (1U) or high-dose (3U)). **A2** Cycle-triggered averages revealed underlying differences in breathing patterns among sham rats and those with acute lung injury. In these examples, the respiratory cycle shortened progressively from sham to higher doses of bleomycin; and the waveform became progressively more similar to a sine wave. **B&C** Respiratory rate (fR) and the coefficient of variation of cycle duration (TTOT) were greater in the bleomycin-treated compared to PBS-treated rats. * = P < 0.05.

mean SampEns of the surrogate data sets did not differ.

3.3.3. Nonlinear Complexity Index (NLCI)

The apparent progressive increase in the difference of SampEn between the original and mean of the surrogate data sets indicate that the nonlinear component of total variability increased with lung injury. We quantified this difference by subtracting the values of SampEn for the original data set from the values for the mean minus the standard deviation of the surrogate data sets (lower dashed gray line in Fig. 4A2); then, dividing the summed differences by the number of τ in which a difference occurred. We refer to this value as the nonlinear complexity index (NLCI). On d0 NLCI did not differ among groups, (PBS, 0.059 ± 0.26, n = 9; 1U, 0.049 ± 0.24, n = 9; 3U, 0.048 ± 0.23, n = 8). On d7 and compared to the rats that received PBS (0.074 ± 0.031 bits), NLCI increased after low- (0.213 ± 0.062 bits, $P < 0.05$) and high- doses of bleomycin rats (0.271 ± 0.107 bits, $P < 0.05$; (Fig. 4C). However, NLCI did not differ between groups receiving low- and high- doses of bleomycin.

3.3.4. NLCI correlated to severity of lung injury

For an index of lung injury we multiplied the protein content of the BALF on d7 by the difference between the expected and the actual weight of the rat on d7 (Fig. 5). We derived this index based on Fig. 2E, in which the change in body weight from d0 to d7 was negatively correlated to the protein concentration in the BALF on d7. The expected body weight was based on growth of the sham group, so subtracting the actual from the expect body weight provided positive numbers. Thus, the product of the difference between expected and actual body weight multiplied by the protein concentration in the BALF should be correlated to severity of lung injury and serve as an index of the severity of lung injury. The strong correlation (r = 0.904) between NLCI and lung injury supports NLCI as a sensitive biometric for lung injury. In a linear regression model, the equation is y = 0.00973x + 0.0567 bits.

3.4. Increased inhaled CO_2 decreased ventilatory pattern variability only in the sham group

In the experimental protocol, we exposed the rats to normoxia (room air), hyperoxia, and then to hyperoxic hypercapnia. The NLCIs did not differ between normoxia and hyperoxia for the sham (0.07 ± 0.03 vs 0.08 ± 0.05; $P > 0.05$); the low-dose (0.18 ± 0.11 vs 0.20 ± 0.10; $P > 0.05$); and for the high dose groups (0.27 ± 0.15 vs 0.24 ± 0.13; $P > 0.05$). Hyperoxic hypercapnia increased NLCI in the sham group (0.19 ± 0.12; $P < 0.05$) but not in the lung injured groups, (1U bleomycin, 0.21 ± 0.10; 3U, 0.26 ± 0.12; Fig. 6)

3.5. Nonlinear measures of ventilatory pattern variability outperformed fR

We applied Receiver Operating Characteristic (ROC) curve analysis (Griner et al., 1981; Zweig and Campbell, 1993) to evaluate the ability of linear and our nonlinear measures to discriminate disease variance in the ventilatory pattern (Fig. 7). We calculated the area under the curves (AUC) to compare the analytical approaches (Fig. 7). Both fR and CV of TTOT were able to identify lung injured rats. CVTTOT had the least sensitivity for a given specificity and consequently, had the lowest area under the curve (AUC = 0.78). In contrast, the nonlinear indices had

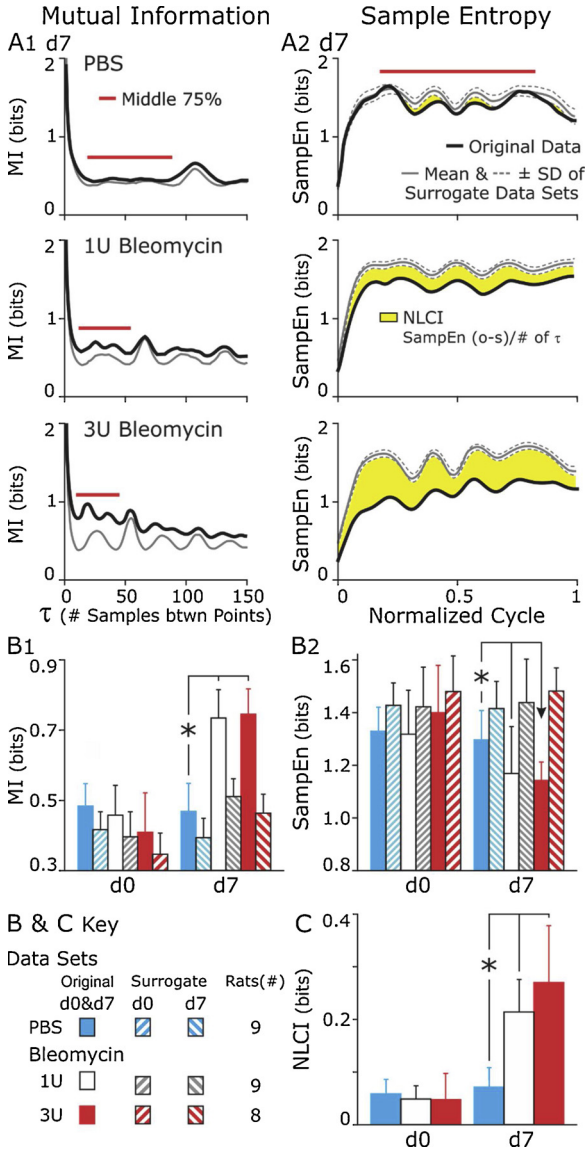

Fig. 4. Nonlinear measures of ventilatory pattern variability. **A1** Representative plots of mutual information (MI) as a function of τ the time lag between points, for each experimental group. Thus, the time lag depended on sampling frequency, which was 200 Hz so 5 ms for τ = 1. As fR increased, the cycle was captured by fewer τ. **A2** Representative plots of sample entropy (SampEn) against τ normalized to one cycle length. As deterministic nonlinear variability becomes a greater component of total variability, MI increased and SampEn decreased in the original datasets; whereas these values remained similar for the surrogate data. **B1** Group data: On d7 after lung injury MI had increased compared to the sham group indicating that the respiratory pattern became more predictable, more stereotypic. **B2** Group data: Consistent with the differences in MI on d7, SampEn had decreased compared to the sham group indicating that patterns in the shaped of the waveform had increased. **C** Group data: For sample entropy we summed differences (highlighted in yellow) between the original data set (black trace) and the surrogate data sets (mean-1 standard deviation, grey dashed trace) and then divided the total by the number of t in which differences occurred. We refer to this value as the nonlinear complexity index (NLCI) because the NLCI reflects the presence of nonlinear contributions to ventilatory pattern variability. The NLCI increased progressively from sham to 1 and 3U of bleomycin indicating a more consistent pattern in the waveform across breaths after lung injury. * = P < 0.05.

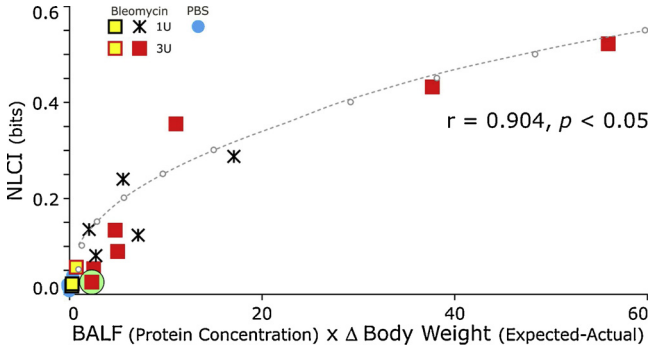

Fig. 5. NLCI, a nonlinear measure of ventilatory pattern variability, correlates highly to the product of BALF protein concentration multiplied by the difference between the expected and actual body weights. The expected body weight was based on the sham group, which gained 47 ± 5.875 g in the week after tracheal instillation of PBS. The three rats identified as sustaining either mild or no lung injury after bleomycin (yellow filled black (1U) or red (3U) boxes) obscure the saline-treated rats (blue circles). The most severely lung injured rats received 3U of bleomycin (red filled boxes), but the moderate range between 2 and 20 had rats that were treated with 1 of 3U of bleomycin.

similar AUC values (MI = 0.94 and NLCI = 0.93) and high sensitivity for a given specificity.

4. Discussion

This study presents an analysis of the nonlinear deterministic properties of the variability in the ventilatory pattern as a diagnostic and predictive strategy. Following ALI the ventilatory waveform becomes more predictable; MI increases and SampEn decreases indicating a loss in VPV. In addition, we utilized surrogate data sets constructed from the original data set to isolate non-linear sources of variability in VPV. These data sets preserve the linear autocorrelation function but destroy the nonlinear deterministic properties of the original data. Thus we calculate a NLCI by comparing the values of sample entropy of the original and surrogate data sets. The ROC supports that NLCI is a diagnostic biometric for distinguishing rats with and without ALI.

4.1. Relevance to neural control of respiration

Our analytic approach revealed a nonlinear, deterministic component to VPV at baseline; and this became a greater part of VPV with increasing severity of lung injury. The presence of deterministic variability indicates that properties of the underlying neural circuitry generating the respiratory pattern relate one breath to the next. The increase in time-dependence in the ventilatory pattern indicates that variability is itself dynamic and perhaps a controlled property of breathing. Our general working hypothesis is that breathing becomes more predictable as a result of brainstem inflammation; evoked by sterile and septic lung injury with the production of damage-associated molecular pattern molecules (DAMPs) and pathogen-associated molecular pattern molecules (PAMPs) respectively (Dhingra et al., 2011; Dick et al., 2013; Jacono et al., 2011; Litvin et al., 2018)).

Deterministic properties were not evident in the reduced neural circuits present in in vitro Pre-Bötzinger Complex even though these small circuits generate a rhythm. Using multiunit recording of spiking activity, a cycle-by-cycle analysis revealed stochastic rather than deterministic variability in the onset of neuronal activity. Specifically, neurons that initiated one cycle would follow in another (Carroll et al., 2013; Carroll and Ramirez, 2013). The authors concluded that each breath was generated by a "*de novo* assembly of a stochastic collaboration of network topology and intrinsic properties". While we have focused on the identified changes in the deterministic variability in the ventilatory waveform, we must note that the sample entropy of the

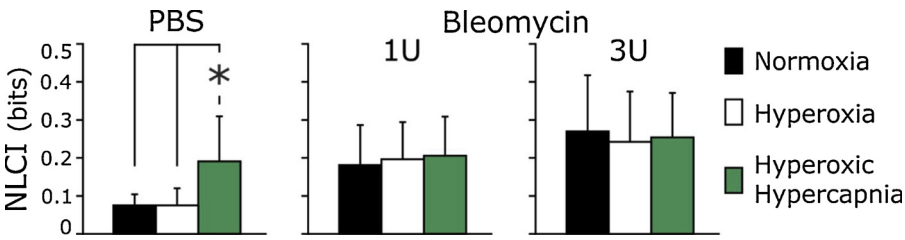

Fig. 6. Summary of the effect of inspired gas on NLCI. Hyperoxia did not impact measurement of NLCI significantly. Hyperoxic hypercapnia increased the NLCI in the sham group but not bleomycin-lung injured rats. In the PBS-treated rats breathing hypercapnia, NLCI became similar to NLCI of bleomycin lung-injured rats. The absence of changes in NLCI in rats with lung injury could indicate a ceiling effect or a mechanism or both. * = P < 0.05.

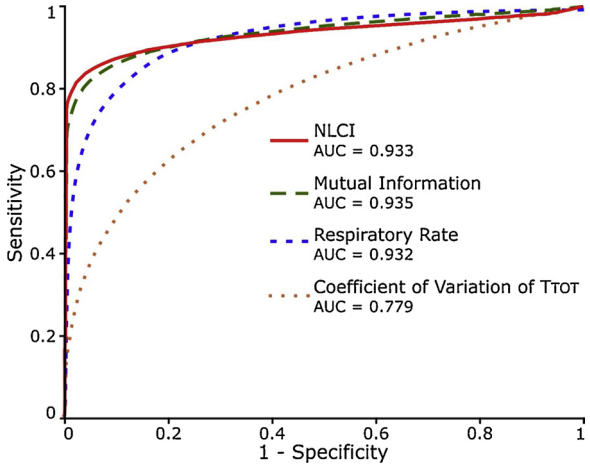

Fig. 7. Receiver operating characteristic (ROC) curves were plotted to compare the diagnostic accuracy of different indices of ventilatory pattern variability for the diagnosis of acute lung injury. The area under the ROC curves (AUC) for CV of TTOT (AUC = 0.78) was the least whereas MI (0.935) and NLCI (0.933) were comparable.

surrogate datasets, which theoretically retains the linear (stochastic) properties of the waveform signals, remained similar before and after lung injury appearing unaffected by brainstem inflammation. Thus, we speculate that the mechanisms modulating VPV after ALI act on nonlinear (deterministic) rather than linear (stochastic) mechanisms.

Our working hypothesis is that synaptic efficacy is affected by brainstem inflammation associated with ALI (Litvin et al., 2018). We recorded evoked excitatory postsynaptic potentials (eEPSCs) from neurons that received monosynaptic glutamatergic input from the *tractus solitarii*. The average amplitude of TS-eEPSC was less in tissue harvested from a juvenile rats a week after ALI compared to that of uninjured rats (Litvin et al., 2018). These data are consistent with decreased responsiveness to sensory input; thus, less variability due to random or transient sensory input. While the details need to be determined, these data support the working hypothesis that brain inflammation affects the nonlinear dynamics of the ventilatory pattern through neural circuits.

Variability of the ventilatory pattern is the final product of the respiratory pattern generator and of sensory, postural and behavioral inputs. In other words, this variability reflects convergence of multiple inputs affecting respiratory pumping and valvular muscles and airways. Convergence of neural activity as well as synchrony of functionally equivalent neurons may act in a circuit to modulate deterministic variability in the ventilatory pattern.

4.2. Magnitude of acute lung injury

Low- and high- doses of bleomycin caused appreciable lung injury, increased respiratory rate, and increased coefficient of variation of TTOT. These changes in the pattern were apparent in the CTAs of airflow. However, the severity of the lung damage varies greatly in and between rodents as models of ALI caused by a single dose of bleomycin. Within a rodent, adjacent areas in the lung can be damage severely or normal (Izbicki et al., 2002). Between animals, both histology and biochemical biomarkers in the BALF are highly variable (Manali et al., 2011; Polosukhin et al., 2005; Ruscitti et al., 2017). Our data reflect this variability in ALI

Due to this variability, we sought an objective measure of the magnitude of the effect bleomycin on the health and well-being of the rats. We reasoned that an index based on the failure of the rats to gain weight like the sham surgical control and on the amount of protein in the BALF would reflect lung damage and its effect on the rat's health. Body weight is a good indicator of rodent health (Hawkins, 2002; Kohn et al., 2007). NIH animal care and use guidelines require measuring body weight at least once a week in monitoring rodents in experimental protocols that occur over an extended period. Further, recent studies using rodent as a preclinical model report that weight loss is correlated to intensity of the exposure to aerosolized ammonia or to imminent death in the days after whole irradiation (Koch et al., 2016; Perkins et al., 2016). Further in a rodent molecular model of cystic fibrosis, weight loss following an intratracheal inoculation with *Pseudomonas aeruginosa* (or sterile) agarose beads was greatest 3 d after infection and was correlated with the inflammatory process rather than with altered pulmonary responsiveness. These studies support using weight loss as a marker of health, in particular associated with lung injury.

Finally, we interpret the increase in predictability in the respiratory waveform in the context of brainstem inflammation but the marked weight loss indicates that hypothalamic inflammation is affecting homeostatic control (Burfeind et al., 2016). The loss of effective connectivity to cardiorespiratory control networks due to inflammation of hypothalamic and other suprapontine inputs must considered as a possible mediator of this effect.

The other variable in our injury index was multiplied the protein content of BALF. In ALI, protein in the alveoli increases due to leaky airway epithelium, pulmonary vascular endothelium cellular debris and the recruitment of cells to the damaged tissue by DAMPs. Given that we collected BALF from three washes of the lung, BALF protein content would average the high protein levels from the damaged areas and low protein levels from the undamaged areas. So even though the damage heterogeneous, the magnitude of overall lung injury would be reflected in BALF.

Thus, it is consistent that NLCI as a biometric for ALI to be highly correlated to an objective measure of the severity of lung injury.

We quantified nonlinear characteristics of the plethysmographic waveform using MI, which measures the probability of knowing a second point given the value of a prior point, and SampEn, which measures the frequency of matches of a third point based on the match of two prior points. Both of these techniques analyze the consistency of the waveform from breath-to-breath (Dhingra et al., 2011).

We developed the nonlinear complexity index (NLCI), which normalizes SampEn to compare SampEn from different epochs and different rats. For the groups, the mean NLCI of the VPV from the rats that received bleomycin was significantly greater than the sham rats. Further, NCLI showed a trend and tended to increase progressively from the sham to low- to high- dose of bleomycin. A priori the number of rats required to test our hypothesis depended on the higher dose of bleomycin to cause greater lung injury consistently. This was not the case. The observed overlap of weight gain (or loss) and the protein concentration of BALF was leveraged to create an index of lung injury

based on weight (the difference between expected (based on the growth of the sham rats) and actual weights) and on the protein concentration of BALF. Using this index, NLCI was highly correlated to the magnitude of lung injury. This was confirmed by receiver operating curve analysis in which nonlinear indexes had a high diagnostic accuracy for ALI.

4.3. Limitations of the analysis

In a similar approach to that applied here, the effectiveness of an assessment algorithm for predicting sepsis was determined by optimizing the area under the under receiver operating characteristic curves (Nemati et al., 2018). In their approach, they analyzed heart rate and arterial blood pressure data. Here, we used primarily the respiratory waveform. Consequently, additional physiologic variables that are monitored like blood gases and body temperature are not considered in development of the tool.

The limitations of a biometric, are its specificity and selectivity. A relevant example is sabermetrics, which refers to analytics developed in part by members of the Society for American Baseball Research (SABRmetrics) (Costa et al., 2007). For instance, since the 19th Century players have been characterized batting average, which treats each at bat equally. Thus, these statistics are independent of the circumstances of the game; such as runners on base and quality of the opposing players. Sabermetrics applies a statistical approach to evaluate a player's performance given the probable outcome of at bat given the game's situation. So like sabermetrics, we are interested in developing statistics based on the situation, in our case, the predictability of the breathing pattern to distinguish subtle but physiologically substantive differences in seriously ill patients to track illness and recovery.

4.3.1. Specificity

Nonlinear measures of the VPV evaluate the mathematical complexity of a complex, integrated behavior, with NLCI greater than 0.075 accurately detecting lung injury. In two rats that received 3U of bleomycin, the product of BALF protein concentration and the difference between predicted and actual body weight was slightly greater than 2.0 indicating mild lung injury. The NLCIs in these two rats were less than 0.075, which would indicate a false negative error. NLCI had a high correlation to the severity of lung injury, as indicated by the protein concentration in the BALF alone and even higher when multiplied by the difference between predicted and actual body weight.

Inhaling hyperoxic hypercapnic gas, evoked a regular breathing pattern that also had NLCI greater than 0.075. In this regard, specificity depends on the patient's history. Further even though hypercapnia increased NLCI in the sham group to that of the injured group, hypercapnia may be acting through a different mechanism. Inhaled CO_2 recruits respiratory-modulated activity in the brainstem and increases central respiratory drive (Cohen, 1968). With a strong drive, the pattern became highly predictable.

4.3.2. Sensitivity

Theoretically, the range of NLCI should be broad, bounded by 0 and the average SampEn of the data but practically it was between 0.01 and 0.55. Further, we plotted a curve for the quadratic regression, which indicates a weak ceiling-effect. A ceiling, or a practical maximal predictability, is also supported by the absence of an increase in NLCI in the injured rats; whereas NCLI increased in sham control rats exposed to increased inhaled carbon dioxide. In our sample entropy analysis we measured a pattern of only three points (m = 3) with a standard tolerance (5%). We have not investigated optimizing these parameters. While NLCI was effective with these standard parameters; optimization of parameters may increase sensitivity without sacrificing specificity.

4.4. ALI changes the breathing pattern

The breathing pattern following lung injury could be due to many factors (Jacono, 2013). In systems engineering terms, the determinants of VPV include: a) the properties of the controller; specifically, the brainstem neurons that generate the respiratory pattern; b) the latency and gain of sensory feedback from chemo-, mechano- and pulmonary edema- receptors; and c) the physical properties of the plant, which includes the airway, pulmonary and chest wall. Which determinants of the breathing pattern are responsible for increasing the predictability of the ventilatory pattern in ALI? In ALI injury to the plant (lungs) is a primary determinant. The physical constraints of the cardiopulmonary system including changes in lung mechanics, interstitial fluid and gas exchange (Jacono et al., 2006; Jubran and Tobin, 2000; Jubran et al., 1997; Fiamma et al., 2007; Van den Aardweg and Karemaker, 2002). Pulmonary edema would activate *J*-receptors, which are innervated vagal C fibers and evoke rapid shallow breathing (Widdicombe, 1982). Reductions in vital capacity (VC) in the setting of gas exchange requirements that necessitate maintenance of a relatively normal tidal volume (V_T) may narrow the VC/V_T ratio and result in a more uniform rate and depth of pattern. However, mechanical properties of the lung are not the sole determinants of breathing patterns (Benchetrit, 2000; Bruce, 1996; Webber and Zbilut, 2006).

In addition to the "plant," the sensors may be altered. The chemoreflex sensitivity or 'gain' of sensory receptors increased following lung injury(Jacono et al., 2006). However, the role of sensory input in affecting VPV is not clear as it can both increase and decrease variability (Dhingra et al., 2017). Further brainstem cytokine expression alters neural processing of afferent feedback; altering the deterministic structure and patterning of respiration after elicited by chemo- and mechano- reflexes (Coles and Dick, 1996; Siniaia et al., 2000). Specifically, pro-inflammatory cytokines are expressed in the nTS after ALI and may decrease in synaptic efficacy of sensory input (Litvin et al., 2018). Thus, the sensory and controller components of the respiratory system are affected by ALI and we are pursuing experiments to elucidate specific causes and mechanisms.

As well as the causes, the physiologic relevance of the ventilatory pattern becoming more predictable is unclear. Changes in the ventilatory pattern may be adaptive or pathogenic. For example, adoption of a breathing pattern with low variability minimizes dyspnea in patients with restrictive lung disease (Brack et al., 2002). In contrast, biologically variable ventilation preserves lung compliance after lung injury (Arold et al., 2002) In summary, we hypothesized that ALI would lead to a change in measured variability based on analyses of VPV in patients recovering from respiratory failure. In our rodent model of ALI, we observed a significant increase in nonlinear determinants of pattern variability.

4.5. Changes in inhaled gases

We addressed the impact of inspired concentrations of oxygen and carbon dioxide on the changes in nonlinear features of the respiratory signal with ALI. The observation that hyperoxia did not reverse the increase in nonlinear complexity suggests that hypoxemia and increased carotid body sensitivity are not the primary drivers of patterning in our animal model. In contrast, hyperoxic hypercapnia leads to significant changes in nonlinear complexity in sham but not ALI rats. These results are consistent with a weak 'ceiling effect,' that is increases in the nonlinear component of variability in the ventilatory pattern was reaching a maximal value. This finding has potential clinical relevance as related to the use of permissive hypercapnia as a ventilatory strategy in patients with ALI/ARDS. Specifically, hypercapnia may mask a reduction of nonlinear variability during recovery.

4.6. Variability of the ventilatory pattern as a biometric

Many prior investigations have measured breathing pattern variability by analyzing cycle duration and tidal volume. For instance, respiratory pattern variability decreases in restrictive lung disease and

increases in COPD. Using measures of the coefficient of variation of tidal volume (CVVT), patients with restrictive lung disease, mean CVVT was less than that of normals; 50% less in one (Kuratomi et al., 1985) and upto 80% less in another study (Brack et al., 2002). In contrast, CVVT almost doubled in patients with obstructive lung disease (Kuratomi et al., 1985). In normal humans, resistive and elastic loads affected expiratory and inspiratory durations (TI and TE) differentially. Depending on the added load, resistive loads increased CVTI and CVTE (Brack et al., 1998) and elastic loads decreased the variability of TE (Brack et al., 1997)

Our analysis considered both respiratory cycles (that is fR and T_{TOT}) and the morphology of the plethysmographic signal. The analysis of the waveform examined the relationship between data points throughout the respiratory cycle to those from one cycle to the next, capturing intra- and inter- breath dynamics. Further, in neural control of the respiration that rhythm (or rate) and pattern (shape of the waveform) are regulated independently (Rybak et al., 2007). That is, the morphology of the waveform may be altered even without a change in respiratory rate, and our analytical approach would be sensitive to this type of change.

In summary, the present study demonstrates that NLCI can quantify change in VPV after lung injury and is highly correlated to the magnitude of the injury. We expect that NLCI will identify decreases in variability due to increases in the predictability of the pattern and such changes occur in sepsis and that increase lung resistance. This result is of potential relevance to strategies for diagnosis and stratification of ALI/ARDS as performed in the emergency department and intensive care unit. In the long term, we envision measures of pattern variability as an “additional vital sign” providing diagnostic and predictive information to clinicians identifying patients in need of a higher level of care or more intensive therapy.

Acknowledgement

We gratefully acknowledge the support of the US Government both the Veteran Affairs Research Service (I01BX004197 & I01BX0008730, Jacono) and National Institutes of Health (U01 EB021960, Dick).

References

Arold, S.P., Mora, R., Lutchen, K.R., Ingenito, E.P., Suki, B., 2002. Variable tidal volume ventilation improves lung mechanics and gas exchange in a rodent model of acute lung injury. Am. J. Respir. Crit. Care Med. 165, 366–371. https://doi.org/10.1164/ajrccm.165.3.2010155.

Atabai, K., Matthay, M.A., 2002. The pulmonary physician in critical care. 5: acute lung injury and the acute respiratory distress syndrome: definitions and epidemiology. Thorax 57, 452–458. https://doi.org/10.1136/THORAX.57.5.452.

Benchetrit, G., 2000. Breathing pattern in humans: diversity and individuality. Respir Physioll 122, 123–129. https://doi.org/10.1016/S0034-5687(00)00154-7.

Brack, T., Jubran, A., Tobin, M.J., 1997. Effect of elastic loading on variational activity of breathing. Am. J. Respir. Crit. Care Med. 155, 1341–1348. https://doi.org/10.1164/ajrccm.155.4.9105077.

Brack, T., Jubran, A., Tobin, M.J., 1998. Effect of resistive loading on variational activity of breathing. Am. J. Respir. Crit. Care Med. 157, 1756–1763. https://doi.org/10.1164/ajrccm.157.6.9704114.

Brack, T., Jubran, A., Tobin, M.J., 2002. Dyspnea and decreased variability of breathing in patients with restrictive lung disease. Am. J. Respir. Crit. Care Med. 165, 1260–1264. https://doi.org/10.1164/rccm.2201018.

Bruce, E.N., 1996. Temporal variations in the pattern of breathing. J. Appl. Physiol. 80, 1079–1087. https://doi.org/10.1152/jappl.1996.80.4.1079.

Burfeind, K.G., Michaelis, K.A., Marks, D.L., 2016. The central role of hypothalamic inflammation in the acute illness response and cachexia. Semin. Cell Dev. Biol. 54, 42–52. https://doi.org/10.1016/j.semcdb.2015.10.038.

Carroll, M.S., Ramirez, J.-M., 2013. Cycle-by-cycle assembly of respiratory network activity is dynamic and stochastic. J. Neurophysiol. 109, 296–305. https://doi.org/10.1152/jn.00830.2011.

Carroll, M.S., Viemari, J.-C., Ramirez, J.-M., 2013. Patterns of inspiratory phase-dependent activity in the in vitro respiratory network. J. Neurophysiol. 109, 285–295. https://doi.org/10.1152/jn.00619.2012.

Cohen, M.I., 1968. Discharge patterns of brain-stem respiratory neurons in relation to carbon dioxide tension. J. Neurophysiol. 31, 142–165. https://doi.org/10.1152/jn.1968.31.2.142.

Coles, S.K., Dick, T.E., 1996. Neurones in the ventrolateral pons are required for post-hypoxic frequency decline in rats. J. Physiol. (Paris) 497, 79–94.

Costa, G.B., Huber, M.R., Saccoman, J.T., 2007. Understanding Sabermetrics: an Introduction to the Science of Baseball Statistics. McFarland & Company, Jefferson, N.C.

Delorme, M.P., Moss, O.R., 2002. Pulmonary function assessment by whole-body plethysmography in restrained versus unrestrained mice. J. Pharmacol. Toxicol. Methods 47, 1–10.

Dhingra, R.R., Jacono, F.J., Fishman, M., Loparo, K.A., Rybak, I.A., Dick, T.E., 2011. Vagal-dependent nonlinear variability in the respiratory pattern of anesthetized, spontaneously breathing rats. J. Appl. Physiol. 111, 272–284. https://doi.org/10.1152/japplphysiol.91196.2008.

Dhingra, R.R., Dutschmann, M., Galán, R.F., Dick, T.E., 2017. Kölliker-Fuse nuclei regulate respiratory rhythm variability via a gain-control mechanism. Am J Physiol-Reg, Int, Comp Physiol 312, R172–R188. https://doi.org/10.1152/ajpregu.00238.2016.

Dick, T.E., Dhingra, R.R., Hsieh, Y.-H., Fishman, M., Kaffashi, F., Loparo, K.A., Wilson, C.G., Jacono, F.J., 2013. Analysis of ventilatory pattern variability. In: Vodovotz, Y., An, G. (Eds.), Complex Systems and Computational Biology Approaches to Acute Inflammation. Springer New York, New York, NY, pp. 79–99. https://doi.org/10.1007/978-1-4614-8008-2_5.

Fiamma, M.-N., Straus, C., Thibault, S., Wysocki, M., Baconnier, P., Similowski, T., 2007. Effects of hypercapnia and hypocapnia on ventilatory variability and the chaotic dynamics of ventilatory flow in humans. Am J Physiol-Regul, Integr Comp Physiol 292, R1985–R1993. https://doi.org/10.1152/ajpregu.00792.2006.

Goldberger, A.L., Amaral, L.A., Hausdorff, J.M., Ivanov, Pc., Peng, C.K., Stanley, H.E., 2002a. Fractal dynamics in physiology: alterations with disease and aging. Proc. Natl. Acad. Sci. U. S. A. 99 (Suppl. 1), 2466–2472. https://doi.org/10.1073/pnas.01257949999/suppl_1/2466. [pii].

Goldberger, A.L., Peng, C.K., Lipsitz, L.A., 2002b. What is physiologic complexity and how does it change with aging and disease? Neurobiol. Aging 23, 23–26 https://doi.org/S0197458001002664 [pii].

Griner, P.F., Mayewski, R.J., Mushlin, A.I., Greenland, P., 1981. Selection and interpretation of diagnostic tests and procedures. Principles and applications. Ann. Intern. Med. 94, 557–592.

Hawkins, P., 2002. Recognizing and assessing pain, suffering and distress in laboratory animals: a survey of current practice in the UK with recommendations. Lab Anmls 36, 378–395.

Hoyer, D., Schmidt, K., Bauer, R., Zwiener, U., Kohler, M., Luthke, B., Eiselt, M., Kiihler, M., Luthke, B., Eiselt, M., 1997. Nonlinear analysis of heart rate and respiratory dynamics. IEEE Eng. Med. Biol. 16, 31–39. https://doi.org/10.1109/51.566150.

Izbicki, G., Segel, M.J., Christensen, T.G., Conner, M.W., Breuer, R., 2002. Time course of bleomycin-induced lung fibrosis. Hip Int. 83, 111–119. https://doi.org/10.1046/j.1365-2613.2002.00220.x.

Jacono, F.J., 2013. Control of ventilation in COPD and lung injury. Respir. Physiol. Neurobiol. 189, 371–376. https://doi.org/10.1016/J.RESP.2013.07.010.

Jacono, F.J., Peng, Y.J., Nethery, D., Faress, J.A., Lee, Z., Kern, J.A., Prabhakar, N.R., 2006. Acute lung injury augments hypoxic ventilatory response in the absence of systemic hypoxemia. J. Appl. Physiol. 101, 1795–1802. https://doi.org/10.1152/japplphysiol.00100.2006. https://doi.org/00100.2006 [pii].

Jacono, F.J., Mayer, C.A., Hsieh, Y.H., Wilson, C.G., Dick, T.E., 2011. Lung and brainstem cytokine levels are associated with breathing pattern changes in a rodent model of acute lung injury. Respir. Physiol. Neurobiol. 178, 429–438. https://doi.org/10.1016/j.resp.2011.04.022. https://doi.org/S1569-9048(11)00160-1 [pii].

Jubran, A., Tobin, M.J., 2000. Effect of isocapnic hypoxia on variational activity of breathing. Am. J. Respir. Crit. Care Med. 162, 1202–1209. https://doi.org/10.1164/ajrccm.162.4.9907003.

Jubran, A., Grant, B.J.B., Tobin, M.J., 1997. Effect of Hyperoxic Hypercapnia on variational activity of breathing. Am J Respir Criti Care Med 156, 1129–1139. https://doi.org/10.1164/ajrccm.156.4.97-01080.

Kaffashi, F., Foglyano, R., Wilson, C.G., Loparo, K.A., 2008. The effect of time delay on approximate & sample entropy calculations. Phys. D Nonlinear Phenom. 237, 3069–3074. https://doi.org/10.1016/j.physd.2008.06.005.

Koch, A., Gulani, J., King, G., Hieber, K., Chappell, M., Ossetrova, N., 2016. Establishment of early endpoints in mouse total-body irradiation model. PLoS One 11, e0161079. https://doi.org/10.1371/journal.pone.0161079.

Kohn, D.F., Martin, T.E., Foley, P.L., Morris, T.H., Swindle, M.M., Vogler, G.A., Wixson, S.K., 2007. Guidelines for the assessment and management of pain in rodents and rabbits. J. Am. Assoc. Lab. Anim. Sci. 46, 97–108.

Kuratomi, Y., Okazaki, N., Ishihara, T., Arai, T., Kira, S., 1985. Variability of breath-by-breath tidal volume and its characteristics in normal and diseased subjects. Ventilatory monitoring with electrical impedance pneumography. Jpn. J. Med. 24, 141–149.

Kurths, J., Voss, A., Saparin, P., Witt, A., Kleiner, H.J., Wessel, N., 1995. Quantitative analysis of heart rate variability. Chaos 5, 88–94. https://doi.org/10.1063/1.166090.

Litvin, D.G., Dick, T.E., Smith, C.B., Jacono, F.J., 2018. Lung-injury depresses glutamatergic synaptic transmission in the nucleus tractus solitarii via discrete age-dependent mechanisms in neonatal rats. Brain Behav. Immun. 70, 398–422. https://doi.org/10.1016/j.bbi.2018.03.031.

Lundblad, L.K.A., Irvin, C.G., Adler, A., Bates, J.H.T., 2002. A reevaluation of the validity of unrestrained plethysmography in mice. J. Appl. Physiol. 93, 1198–1207. https://doi.org/10.1152/japplphysiol.00080.2002.

Malik, M., 1996. Heart rate variability Standards of measurement, physiological interpretation, and clinical use. Eur. Hear. J 17, 354–381.

Manali, E.D., Moschos, C., Triantafillidou, C., Kotanidou, A., Psallidas, I., Karabela, S.P., Roussos, C., Papiris, S., Armaganidis, A., Stathopoulos, G.T., Maniatis, N.A., 2011. Static and dynamic mechanics of the murine lung after intratracheal bleomycin. BMC Pul. Med. 11 (33). https://doi.org/10.1186/1471-2466-11-33.

Nemati, S., Holder, A., Razmi, F., Stanley, M.D., Clifford, G.D., Buchman, T.G., 2018. An interpretable machine learning model for accurate prediction of sepsis in the ICU. Crit. Care Med. 46, 547–553. https://doi.org/10.1097/CCM.0000000000002936.

Nirogi, R., Shanmuganathan, D., Jayarajan, P., Abraham, R., Kancharla, B., 2012. Comparison of whole body and head out plethysmography using respiratory stimulant and depressant in conscious rats. J. Pharm. Toxicol. Meth. 65, 37–43. https://doi.org/10.1016/J.VASCN.2011.10.001.

Papaioannou, V.E., Chouvarda, I.G., Maglaveras, N.K., Pneumatikos, I.A., 2011. Study of multiparameter respiratory pattern complexity in surgical critically ill patients during weaning trials. BMC Physiol. 11, 2. https://doi.org/10.1186/1472-6793-11-2.

Peng, C.-K., Mietus, J.E., Liu, Y., Lee, C., Hausdorff, J.M., Stanley, H.E., Goldberger, A.L., Lipsitz, L.A., 2002. Quantifying fractal dynamics of human respiration: age and gender effects. Ann. Biomed. Eng. 30, 683–692. https://doi.org/10.1114/1.1481053.

Perkins, M.W., Wong, B., Tressler, J., Coggins, A., Rodriguez, A., Devorak, J., Sciuto, A.M., 2016. Assessment of inhaled acute ammonia-induced lung injury in rats. EBSCOhost. Inhal. Toxicol. 28, 71–79. https://doi.org/10.3109/08958378.2015.1136715.

Phua, J., Badia, J.R., Adhikari, N.K.J., Friedrich, J.O., Fowler, R.A., Singh, J.M., Scales, D.C., Stather, D.R., Li, A., Jones, A., Gattas, D.J., Hallett, D., Tomlinson, G., Stewart, T.E., Ferguson, N.D., 2009. Has mortality from acute respiratory distress syndrome decreased over time?: a systematic review. Am. J. Resp. Crit. Care Med. 179, 220–227. https://doi.org/10.1164/rccm.200805-722OC.

Polosukhin, V.V., Stathopoulos, G.T., Lawson, W.E., Blackwell, T.S., 2005. Variability of interalveolar septal remodeling after bleomycin treatment in mice. Ultrastruct. Path. 29, 53–64. https://doi.org/10.1080/019131290882286.

Richman, J.S., Moorman, J.R., 2000. Physiological time-series analysis using approximate entropy and sample entropy. Am. J. Physiol.-Heart Circ. Physiol. 278, H2039–H2049. https://doi.org/10.1152/ajpheart.2000.278.6.H2039.

Ruscitti, F., Ravanetti, F., Essers, J., Ridwan, Y., Belenkov, S., Vos, W., Ferreira, F., KleinJan, A., van Heijningen, P., Van Holsbeke, C., Cacchioli, A., Villetti, G., Stellari, F.F., 2017. Longitudinal assessment of bleomycin-induced lung fibrosis by Micro-CT correlates with histological evaluation in mice. Multidiscip. Respir. Med. 12, 8. https://doi.org/10.1186/s40248-017-0089-0.

Rybak, I.A., Abdala, A.P.L., Markin, S.N., Paton, J.F.R., Smith, J.C., 2007. Spatial organization and state-dependent mechanisms for respiratory rhythm and pattern generation. Prog. Brain Res. 165, 201–220. https://doi.org/10.1016/S0079-6123(06)65013-9.

Schreiber, T., Schmitz, A., 1996. Improved surrogate data for nonlinearity tests. Phys. Rev. Lett. 77, 635–638. https://doi.org/10.1103/PhysRevLett.77.635.

Schreiber, T., Schmitz, A., 2000. Surrogate time series. Phys. D 142, 346–382. https://doi.org/10.1016/S0167-2789(00)00121-4.

Seely, A.J.E., Macklem, P.T., 2004. Complex systems and the technology of variability analysis. Crit Care 8, R367. https://doi.org/10.1186/cc2948.

Seely, A.J.E., Bravi, A., Herry, C., Green, G., Longtin, A., Ramsay, T., Fergusson, D., McIntyre, L., Kubelik, D., Maziak, D.E., Ferguson, N., Brown, S.M., Mehta, S., Martin, C., Rubenfeld, G., Jacono, F.J., Clifford, G., Fazekas, A., Marshall, J., 2014. Do heart and respiratory rate variability improve prediction of extubation outcomes in critically ill patients? Crit Care 18, R65. https://doi.org/10.1186/cc13822.

Siniaia, M.S., Young, D.L., Poon, C.-S., 2000. Habituation and desensitization of the Hering-Breuer reflex in rat. J. Physiol. (Paris) 523, 479–491. https://doi.org/10.1111/j.1469-7793.2000.t01-1-00479.x.

Tobin, M.J., 1992. Breathing pattern analysis. Intensive Care Med. 18, 193–201.

Tobin, M.J., Chadha, T.S., Jenouri, G., Birch, S.J., Gazeroglu, H.B., Sackner, M.A., 1983a. Breathing patterns. 1. Normal subjects. Chest 84, 202–205.

Tobin, M.J., Chadha, T.S., Jenouri, G., Birch, S.J., Gazeroglu, H.B., Sackner, M.A., 1983b. Breathing patterns. 2. Diseased subjects. Chest 84, 286–294.

Van den Aardweg, J.G., Karemaker, J.M., 2002. Influence of chemoreflexes on respiratory variability in healthy subjects. Am. J. Respir. Crit. Care Med. 165, 1041–1047. https://doi.org/10.1164/ajrccm.165.8.2104100.

Vandendriessche, B., Abas, M., Dick, T.E., Loparo, K.A., Jacono, F.J., 2017. A framework for patient state tracking by classifying multiscalar physiologic waveform features. IEEE Trans. Biomed. Eng. 1–1https://doi.org/10.1109/TBME.2017.2684244. in press.

Voss, A., Kurths, J., Kleiner, H.J., Witt, A., Wessel, N., 1995. Improved analysis of heart rate variability by methods of nonlinear dynamics. J. Electrocardiol. 28 (Suppl), 81–88. https://doi.org/10.1016/S0022-0736(95)80021-2.

Webber, C.L., Zbilut, J.P., 2006. Ventilatory pattern variability in mammals. Wiley Encyclopedia of Biomedical Engineering. John Wiley & Sons, Inc, Hoboken, NJ, USA, pp. 1–7. https://doi.org/10.1002/9780471740360.ebs1260.

Weil, P., Hoffgaard, F., Hamacher, K., 2009. Estimating sufficient statistics in co-evolutionary analysis by mutual information. Comput. Biol. Chem. 33, 440–444. https://doi.org/10.1016/J.COMPBIOLCHEM.2009.10.003.

Widdicombe, J.G., 1982. Pulmonary and respiratory tract receptors. J. Exp. Biol. 100, 41–57.

Zweig, M.H., Campbell, G., 1993. Receiver-operating Characteristic (ROC) Plots: A Fundamental.